

Ionic Group-Dependent Structure of Complex Coacervate Hydrogels Formed by ABA Triblock Copolymers

Seyoung Kim,^{1,†} Jung-Min Kim,^{1,†} Kathleen Wood,² and Soo-Hyung Choi^{1,*}

¹Department of Chemical Engineering, Hongik University, Seoul 04066, Republic of Korea

²Australian Centre for Neutron Scattering, Australian Nuclear Science and Technology
Organisation, Lucas Heights, NSW 2234, Australia

†These authors contributed equally to this work.

*Author for correspondence: shchoi@hongik.ac.kr

Molecular Characterizations

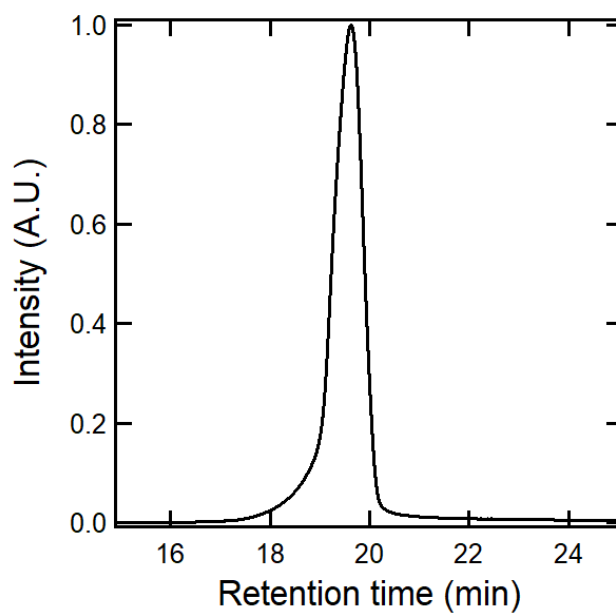


Figure S1. SEC trace of PAGE-*b*-PEO-*b*-PAGE triblock copolymer ($M_{n,PEO} = 20$ kg/mol and $M_{n,end} = 5.0$ kg/mol). SEC was run in chloroform with a refractive index (RI) detector and calibrated using a PS standard.

Critical Salt Concentrations

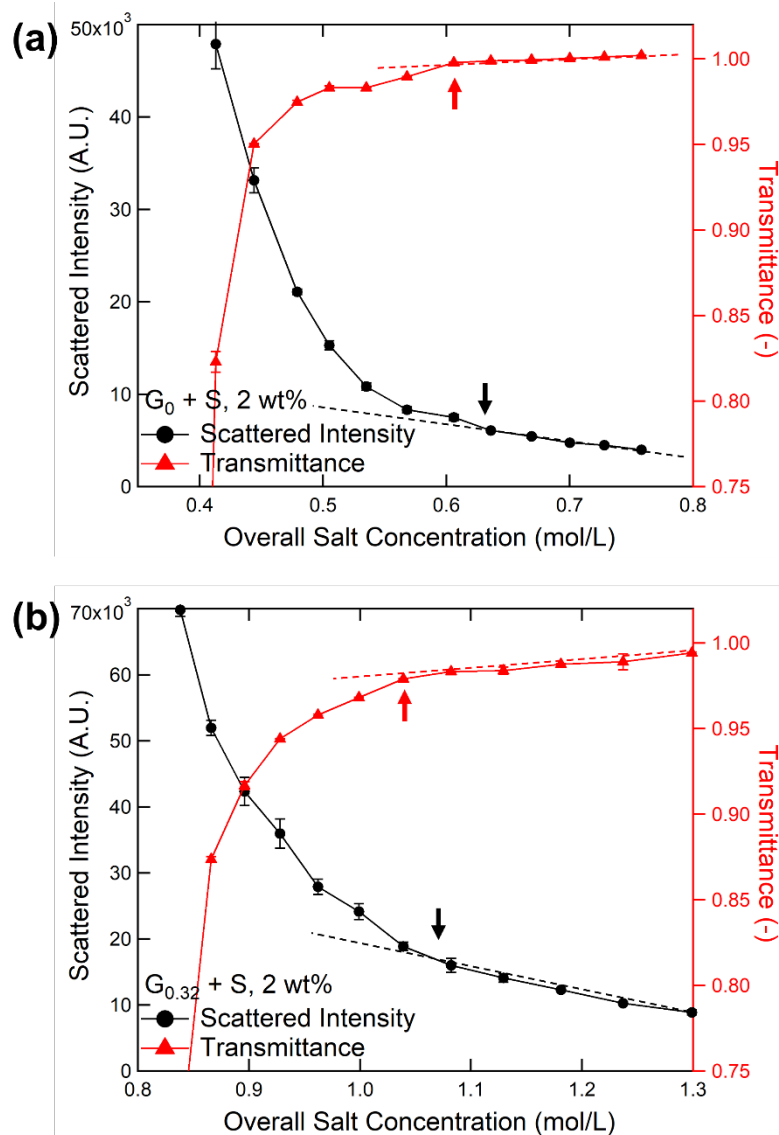


Figure S2. Scattered light intensities and normalized transmission of (a) $G_0 + S$ and (b) $G_{0.32} + S$ as functions of overall salt concentration measured at 2 wt% polymer concentrations. The dashed lines are guides to eye. The ranges of the critical salt concentrations were determined from the points (the arrows) where the scattered intensity or the normalized transmission diverge from the high-salt linearity trends.

Scattering Length Densities (SLDs)

Quantitative model fitting of small-angle X-ray and neutron scattering (SAX/NS) data requires precise values of scattering length densities (SLDs).¹ Both can be calculated from the elemental composition and the molecular volume (v) of the molecules,

$$\rho_{(X/N)} = \frac{\sum_{i=1}^n b_i}{v} \quad (\text{S1}),$$

where X and N in the subscripts are designated for X-ray and neutron, respectively, and b_i is the scattering length of the i -th atom composing the molecule of total n atoms.¹ For X-ray, $b_{i,X}$ is defined as $b_{i,X} = Z_i r_e$, where Z_i is the atomic number of the i -th atom and $r_e = 2.81 \times 10^{-13}$ cm is the electron radius. For neutron, $b_{i,N}$ is the bound coherent scattering length of the i -th atom, where “bound” atom means that the molecule is in a condensed state of matter.

For a multi-molecular homogeneous phase such as a polymer solution, SLDs are the volume average of the components’ SLDs with regard to the partial molecular volume (v_j) of the j -th molecule,²

$$\rho_{(X/N)} = \phi_A \frac{(\sum_{i=1}^n b_i)_A}{v_A} + \phi_B \frac{(\sum_{i=1}^n b_i)_B}{v_B} + \dots \quad (\text{S2}).$$

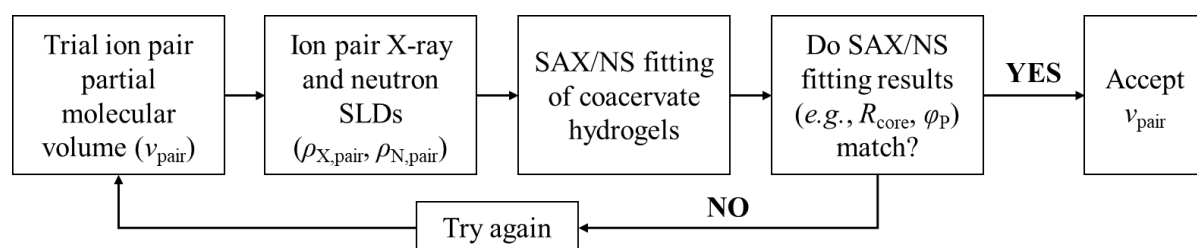
When the actual partial molecular volumes are not known, v_j is generally assumed as the molecular volume of the j -th molecule in its pure state. While the assumption works well for nearly ideal mixtures, it fails on strongly non-ideal mixture where the volume change of mixing is significant. Since polyelectrolyte complex coacervates are concentrated with polyelectrolyte molecules and strong ternary interactions among polyelectrolytes of opposite charges and water are present,³ polyelectrolyte complex coacervates are expected to deviate from the ideality in a great extent. Therefore, the actual partial volumes should be assessed for the appropriate estimation of SLDs.

For the present, we modeled the SLDs of coacervate phase as follows:

$$\rho_{c(X/N)} = \varphi_P \frac{\beta_{pair}(x_D)}{v_{pair}} + (1 - \varphi_P) \rho_{s(X/N)}(x_D) \quad (S3),$$

where φ_P is the fraction of volume occupied by both polyelectrolytes in the coacervate phase, v_{pair} is the partial molecular volume of the “ion pair”, *i.e.*, a pair of cationic and anionic monomers excluding the counterions, $\beta_{pair}(x_D) = (\sum_{i=1}^n b_i(x_D))_{pair}$ is the scattering length of an ion pair, $\rho_s(x_D)$ is the SLD of solvent, and x_D is the volume fraction of D₂O in overall solvent. Here, the scattering length, $b_i(x_D)$, is a function of x_D since the ammonium (NH₃⁺) and guanidinium (CN₃H₅⁺) groups in the positively charged polyelectrolyte can exchange hydrogens with the solvent medium. Furthermore, we make several underlying assumptions: (i) φ_P is independent of x_D since the isotopic composition of water and charged groups does not affect the coacervation equilibrium; (ii) v_{pair} is independent of x_D because the atomic volume of H and D is nearly identical; (iii) the hydrogens in ammonium and guanidinium side-groups undergo complete exchange with the medium, which is supported from earlier protein studies;^{2,4} (iv) in case of the salt addition, the salt concentration relative to the water volume fraction is nearly constant throughout the coacervate and the supernatant phases;³ and (v) the partial volume of water is the same as the volume of pure water (analogous to the Raoult’s law), because water comprises >50 vol% of the coacervate phases. It is noted that the actual isotopic effect on the coacervation equilibrium (*e.g.*, coacervates formed in H₂O vs. D₂O) remains unexplored yet; however, the negligible differences between the dielectric constants of H₂O and D₂O and between the pK_a values of charged groups present in polyelectrolytes (*i.e.*, ammonium, guanidinium, and sulfonate polymers) in H₂O and D₂O,^{5,6} and the negligible isotopic effect on the electrostatic interactions⁷ support the negligible effect of deuterium content in the coacervation equilibrium.

The conventional measurement of partial volume of each component relies on the pycnometry, where a component of small quantity is added in a large vessel of the mixture and the subsequent change in total volume is tracked. However, this method cannot be applied to complex coacervates, since the addition of component, either water or polyelectrolytes, drives into new equilibrium of phase separation. We developed an alternative method to estimate the partial molecular volume of the “ion pair” (v_{pair}) by employing the simultaneous model fitting to SAX/NS of the coacervate core hydrogels used in this work. The flowchart below describes the process of finding v_{pair} that gives the closest matching between SAX/NS data fitting results through conjectured ion pair SLDs for SAX/NS ($\rho_{\text{X/N,pair}}$), where $\rho_{\text{X/N,pair}}(x_{\text{D}}) = \beta_{\text{X/N,pair}}(x_{\text{D}})/v_{\text{pair}}$.



The model function for SAX/NS profiles was adopted from Pedersen *et al.*⁸ and contains fitting parameters including the core radius (R_{core}), the effective hard-sphere radius (R_{hs}), the corona shape factors (a and s), and ϕ_{P} . The detailed fitting model and fitting process are described in the following section, and the results are summarized in Table S1 and S2. A satisfactory results from the model fitting as presented in Figure S3 and a good agreement between the fitting results from SAX/NS measurements, particularly the core structure (i.e., R_{core} and ϕ_{P}), were obtained with $\rho_{\text{G,pair}} = 1.4 \text{ g/cm}^3$ for both $\text{G}_0 + \text{S}$ and $\text{G}_{0.95} + \text{S}$ hydrogels, which corresponds to $v_{\text{pair}} = 548$ and 598 \AA^3 , respectively. This conjectured quantity also agrees with the previously reported SLD value of $1.18 \times 10^{-6} \text{ \AA}^{-2}$ at the SLD-matching point of $x_{\text{D}} = 0.25$ (It is noted that the SLD can vary with the D_2O fraction owing to the hydrogen/deuterium

exchange),⁹ since the recalculation of $G_{0.95} + S$ coacervate using $v_{\text{pair}} = 598 \text{ \AA}^3$ gives a neutron SLD of $\rho_{N,\text{pair}} = 1.20 \times 10^{-6} \text{ \AA}^{-2}$ at $x_D = 0.25$. The results of $\rho_{X,\text{pair}}$, and $\rho_{N,\text{pair}}$ for all $G_x + S$ ion pairs summarized in Table 1 in the main text.

Table S1. Structural parameters of the $G_0 + S$ C3Gs at 0 M NaCl using trial v_{pair} .

$v_{\text{pair}} [10^2 \text{ \AA}^3]$ ($\rho_{G,\text{pair}} [\text{g}/\text{cm}^3]$)	Instrument	$R_{\text{core}} [\text{\AA}]$	$\phi_P [-]$	$R_{\text{hs}} [\text{\AA}]$	$a [-]$	$s [-]$
5.90	SAXS	65 ± 13	0.58	143	0.31	116
(1.30)	SANS	77 ± 10	0.38	146	0.22	122
5.68	SAXS	70 ± 13	0.45	144	-0.06	108
(1.35)	SANS	76 ± 10	0.38	146	0.29	126
5.48	SAXS	74 ± 13	0.37	145	-0.23	108
(1.40)	SANS	75 ± 10	0.39	146	0.38	131
5.29	SAXS	78 ± 13	0.31	146	-0.35	105
(1.45)	SANS	74 ± 10	0.40	146	0.46	134

Table S2. Structural parameters of the $G_{0.95} + S$ C3Gs at 0 M NaCl using trial v_{pair} .

$v_{\text{pair}} [10^2 \text{ \AA}^3]$ ($\rho_{G,\text{pair}} [\text{g}/\text{cm}^3]$)	Instrument	$R_{\text{core}} [\text{\AA}]$	$\phi_P [-]$	$R_{\text{hs}} [\text{\AA}]$	$a [-]$	$s [-]$
6.20	SAXS	65 ± 6	0.89	157	-0.27	52
(1.35)	SANS	73 ± 7	0.62	153	0.27	122
5.98	SAXS	71 ± 6	0.66	157	0.37	83
(1.40)	SANS	72 ± 7	0.64	154	0.38	128
5.77	SAXS	74 ± 6	0.56	157	0.09	91
(1.45)	SANS	70 ± 7	0.66	155	0.50	133
5.58	SAXS	77 ± 6	0.48	157	-0.07	98
(1.50)	SANS	69 ± 7	0.69	155	0.61	134

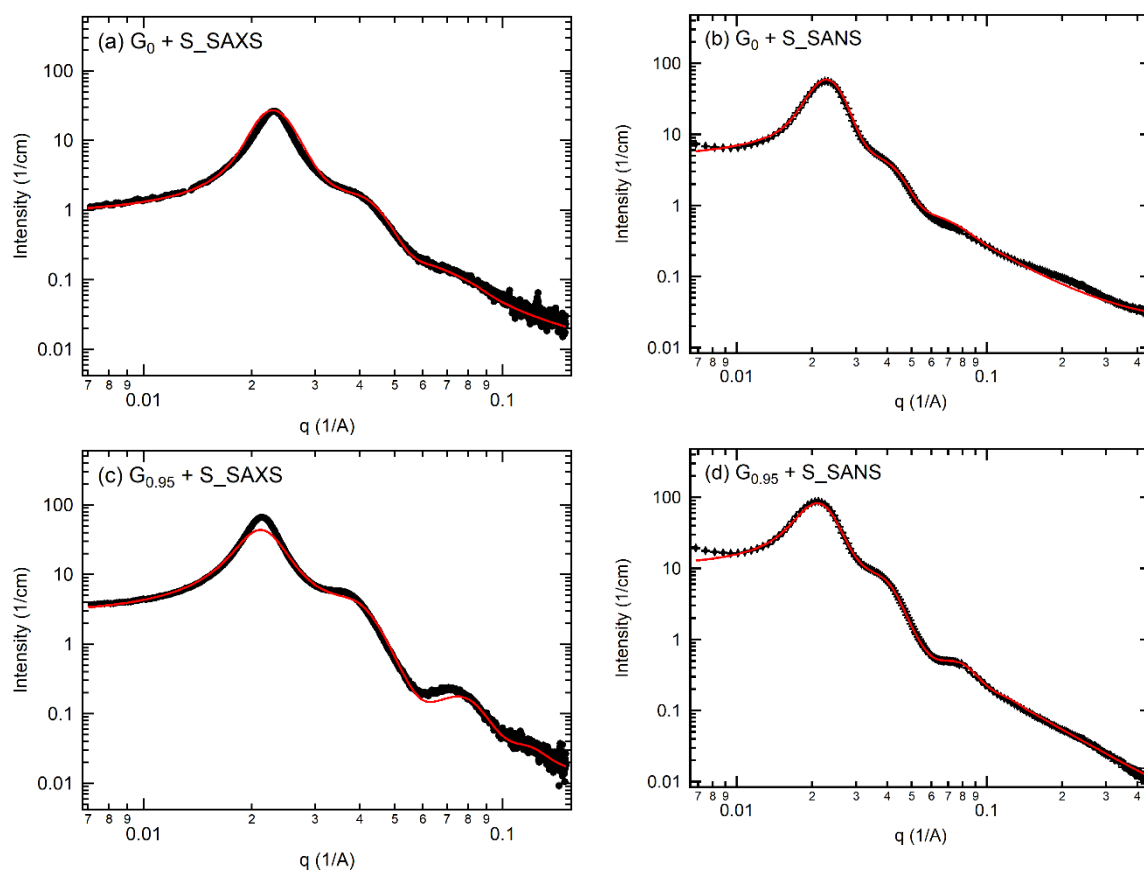


Figure S3. Representative profiles of SAXS and SANS using (a, b) $G_0 + S$ and (c, d) $G_{0.95} + S$ hydrogels at 0 M NaCl. Red solid lines denote the model fitting.

Small-Angle Scattering Model for Coacervate Core Hydrogels.

The SAX/NS profiles of coacervate-core hydrogels from triblock copolyelectrolyte were adjusted by the detailed fitting model given by Pedersen *et al.*,⁸ where the coacervate cores are modelled as spheres and the PEO midblock as polymer brushes attached to the core surface. All contributions from the “micellar structure”, *i.e.*, the core and the PEO corona chains, are considered to model the scattering from a single micelle,

$$P_{\text{mic}}(q) = [N_{\text{agg}}\beta_{\text{core}}A_{\text{core}}(q)]^2 + 2N_{\text{agg}}^2\beta_{\text{core}}\beta_{\text{corona}}A_{\text{core}}(q)A_{\text{corona}}(q) + N_{\text{agg}}\beta_{\text{corona}}^2P_{\text{corona}}(q) + N_{\text{agg}}(N_{\text{agg}} - 1)[\beta_{\text{corona}}A_{\text{corona}}(q)]^2 \quad (\text{S4}),$$

where q is the scattering vector, $N_{\text{agg}} = (4\pi/3)\phi_{\text{P}}R_{\text{core}}^3/\nu_{\text{core}}$ is the aggregation number defined as the number of polyelectrolyte pairs comprising the core, and β_i is the total excess scattering length of species i (either the core or the corona chain) defined as $\beta_i = \nu_i(\rho_i - \rho_s)$. Here, ν_i is the partial molecular volume of the chain i , ρ_i is the SLD of species i , and ρ_s is the SLD of solvent medium. Furthermore, $\nu_{\text{core}} = N_{\text{end}}\nu_{\text{pair}}$ and $\nu_{\text{corona}} = N_{\text{EO}}\nu_{\text{EO}}$ were implemented, where $N_{\text{end},+} = N_{\text{end},-} = N_{\text{end}}$ is the number of repeat units in polyelectrolyte end block, N_{EO} is the repeat units in PEO midblock, and ν_{EO} the partial molecular volume per repeat unit in PEO.

The first term in eq S4 is the self-correlation of the spherical core with the radius R_{core} and width of the core-corona interface σ_{int} at which SLD smoothly decays. The normalized scattering amplitude of the core, $A_{\text{core}}(q)$, is given as

$$A_{\text{core}}(q) = \Phi(qR_{\text{core}}) \exp(-q^2\sigma_{\text{int}}^2/2) \quad (\text{S5}),$$

where $\Phi(x) = 3x^{-3}(\sin x - x \cos x)$ is the Fourier transformed solid sphere. The second term in eq S4 is the cross-correlation between the core and the corona chains with the normalized Fourier transform of the radial density distribution function of the corona,

$$A_{\text{corona}}(q) = \frac{4\pi \int \varphi_{\text{corona}}(r) \frac{\sin(qr)}{qr} r^2 dr}{4\pi \int \varphi_{\text{corona}}(r) r^2 dr} \exp(-q^2 \sigma_{\text{int}}^2/2) \quad (\text{S6}),$$

assuming the radial symmetry of the corona density profile, $\varphi_{\text{corona}}(r)$. A number of models have been proposed to describe the real behavior of $\varphi_{\text{corona}}(r)$.^{8,11} In this work, a linear combination of two cubic b spline functions with two fitting parameters (namely, a and s) was chosen for its simplicity. The last two terms in eq S4 are the self- and cross-correlations within the corona domain, where the chain form factor, $P_{\text{corona}}(q)$, is approximated by the Debye function for a Gaussian chain with radius of gyration R_g ,

$$P_{\text{corona}}(q) = 2x^{-2} (\exp(-x) - 1 + x) \quad (\text{S7}),$$

with $x = q^2 R_g^2$.

The total scattering intensity is expressed using the independent scattering by individual micelles and the hard-sphere inter-micellar structure factor $S(q)$,

$$I(q) = P_{\text{mic}}(q) + A_{\text{mic}}(q)^2 [S(q) - 1] \quad (\text{S8}),$$

where $A_{\text{mic}}(q)$ is the scattering amplitude of the radial scattering length distribution of the micelle,

$$A_{\text{mic}}(q) = N_{\text{agg}} [\beta_{\text{core}} A_{\text{core}}(q) + \beta_{\text{corona}} A_{\text{corona}}(q)] \quad (\text{S9}).$$

The structure factor is characterized by two additional fitting parameters, namely, the hard sphere radius (R_{hs}) and volume fraction (η_{hs}). Lastly, to account for polydispersity in micelle size, a Gaussian distribution for the core radius, $D(R_{\text{core}})$, is employed. The total scattering intensity for the polydisperse model is given as

$$I(q) = \int D(R_{\text{core}}) [P_{\text{mic}}(q; R_{\text{core}}) + A_{\text{mic}}(q; R_{\text{core}})^2 [S(q) - 1]] dR_{\text{core}} \quad (\text{S10}),$$

where the Gaussian distribution $D(R_{\text{core}})$ is parameterized with the average radius $\langle R_{\text{core}} \rangle$ and

the standard deviation σ_R and truncated at $R_{\text{core}} = 0$ for the calculation. It is noted that N_{agg} involved in $P_{\text{mic}}(q; R_{\text{core}})$ (eq S4) and $A_{\text{mic}}(q; R_{\text{core}})$ (eq S9) is also a function of R_{core} . Therefore, total 8 parameters were adjusted during the curve fitting: φ_P , $\langle R_{\text{core}} \rangle$, σ_R , σ_{int} , a , s , R_g , and R_{hs} . η_{hs} was back-calculated from the polymer weight concentration (c) via

$$\eta_{\text{hs}} = (4\pi/3)cR_{\text{hs}}^3/N_{\text{agg}}(v_{\text{core}} + v_{\text{corona}}) \quad (\text{S11}).$$

The fitting range was $0.008 < q \text{ (\AA}^{-1}\text{)} < 0.15$ for SANS and $0.009 < q \text{ (\AA}^{-1}\text{)} < 0.4$ for SAXS. Both SAX/NS profiles were absolute scaled using proper standard calibrations and then fitted using eq S10. The fitting routine was developed in-house and implemented in Igor Pro software. The SANS fitting was accompanied with smearing function which accounts for the neutron wavelength dispersion.

SAX/NS Fitting Results

Table S3. Structural parameters of C3Gs at $c_{\text{NaCl}} = 0$ M.

Sample code	Instrument	R_{core} [Å]	ϕ_{P} [-]	R_{hs} [Å]	η_{hs} [-]	N_{agg} [-]
G ₀ + S	SAXS	72 ± 12	0.41	143	0.49	58
	SANS	74 ± 10	0.40	145	0.49	59
G _{0.32} + S	SAXS	70 ± 11	0.51	146	0.46	63
	SANS	73 ± 8	0.51	150	0.45	69
G _{0.49} + S	SAXS	74 ± 9	0.51	157	0.50	72
	SANS	73 ± 7	0.57	153	0.44	76
G _{0.76} + S	SAXS	75 ± 9	0.55	158	0.46	79
	SANS	71 ± 8	0.58	150	0.44	70
G _{0.95} + S	SAXS	72 ± 8	0.62	151	0.41	77
	SANS	72 ± 7	0.64	154	0.43	77

Table S4. Structural parameters of C3Gs at $c_{\text{NaCl}} = 0.2$ M.

Sample code	Instrument	R_{core} [Å]	ϕ_{P} [-]	R_{hs} [Å]	η_{hs} [-]	N_{agg} [-]
G ₀ + S	SAXS	62 ± 14	0.34	112	0.43	23
	SANS	60 ± 11	0.33	119	0.46	27
G _{0.32} + S	SAXS	61 ± 13	0.44	119	0.42	38
	SANS	65 ± 9	0.50	137	0.44	49
G _{0.49} + S	SAXS	67 ± 11	0.49	137	0.46	53
	SANS	70 ± 9	0.54	145	0.44	65
G _{0.76} + S	SAXS	66 ± 11	0.52	138	0.46	53
	SANS	71 ± 8	0.57	149	0.44	69
G _{0.95} + S	SAXS	71 ± 9	0.58	148	0.43	70
	SANS	73 ± 7	0.62	155	0.42	79

Table S5. Structural parameters of C3Gs at $c_{\text{NaCl}} = 0.4$ M.

Sample code	Instrument	R_{core} [Å]	φ_{P} [-]	R_{hs} [Å]	η_{hs} [-]	N_{agg} [-]
G ₀ + S	SAXS	56 ± 15	0.31	95	0.38	16
	SANS	58 ± 15	0.30	100	0.41	24
G _{0.32} + S	SAXS	60 ± 13	0.40	115	0.44	29
	SANS	62 ± 12	0.42	120	0.44	38
G _{0.49} + S	SAXS	65 ± 12	0.44	128	0.45	44
	SANS	64 ± 10	0.52	130	0.42	49
G _{0.76} + S	SAXS	65 ± 11	0.53	136	0.46	51
	SANS	67 ± 10	0.57	139	0.42	59
G _{0.95} + S	SAXS	68 ± 11	0.56	139	0.41	60
	SANS	73 ± 7	0.61	155	0.43	78

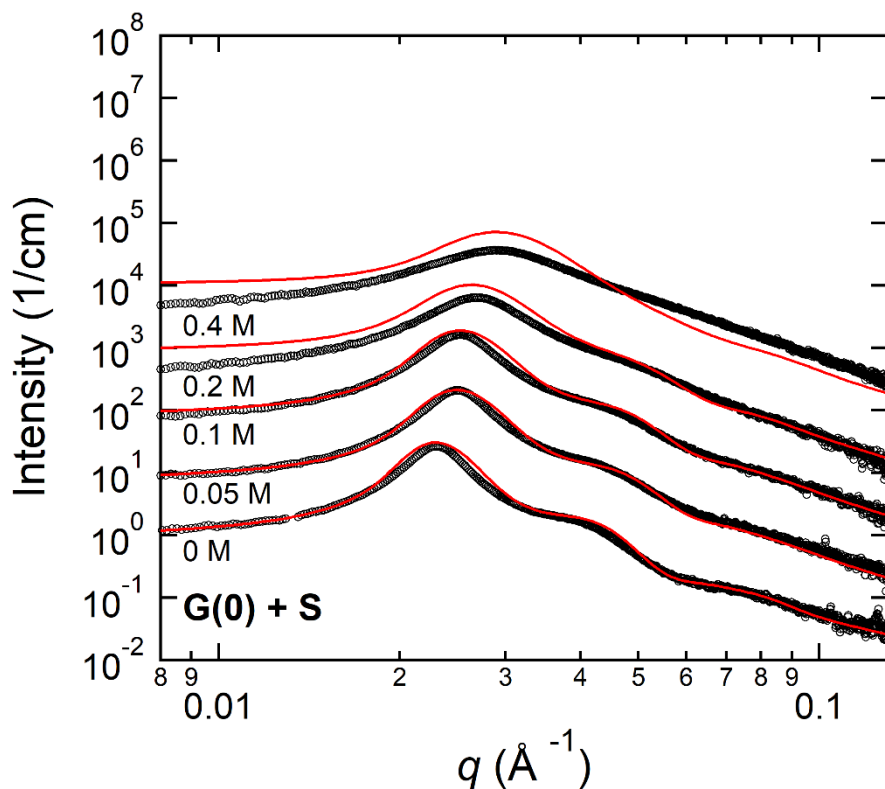


Figure S4. SAXS profiles obtained from $G_0 + S$ hydrogels at various c_{NaCl} . Red solid lines denote the model fitting.

Table S6. Structural parameters obtained from SAXS of the $G_0 + S$ hydrogels.

c_{NaCl} [M]	R_{core} [Å]	φ_{P} [-]	R_{hs} [Å]	η_{hs} [-]	N_{agg} [-]
0	72 ± 12	0.41	143	0.49	58
0.05	66 ± 13	0.39	129	0.48	44
0.1	65 ± 13	0.39	126	0.47	42
0.2	62 ± 14	0.34	112	0.43	32
0.4	56 ± 15	0.31	95	0.38	23

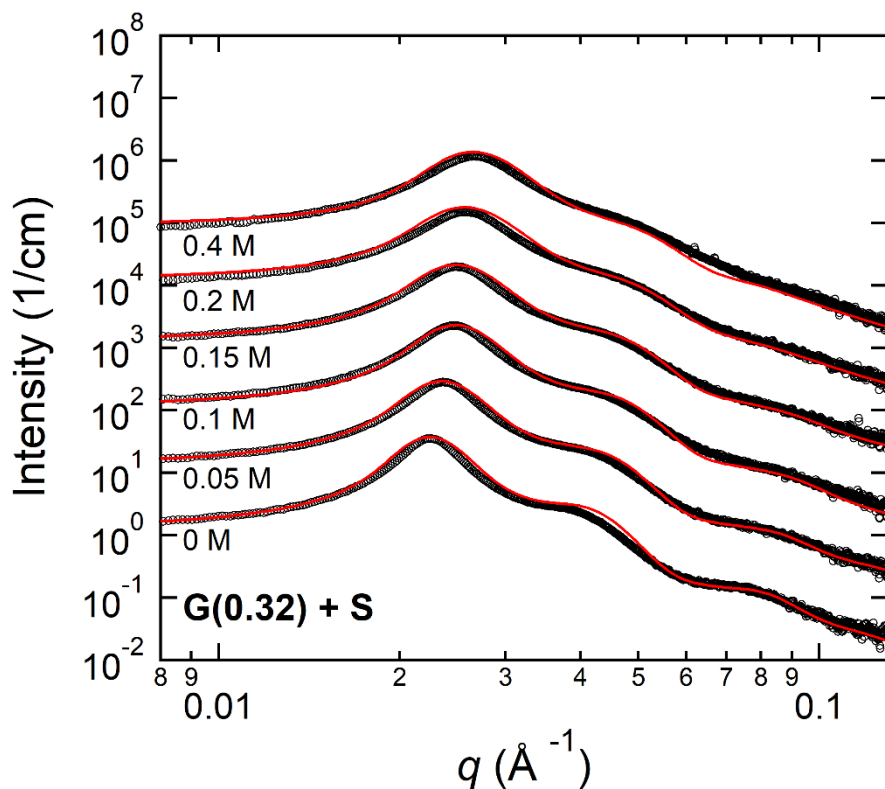


Figure S5. SAXS profiles obtained from $G_{0.32} + S$ hydrogels at various c_{NaCl} . Red solid lines denote the model fitting.

Table S7. Structural parameters obtained from SAXS of the $G_{0.32} + S$ hydrogels.

c_{NaCl} [M]	R_{core} [Å]	φ_{P} [-]	R_{hs} [Å]	η_{hs} [-]	N_{agg} [-]
0	70 ± 11	0.51	146	0.46	63
0.05	66 ± 13	0.51	136	0.43	55
0.1	63 ± 11	0.49	128	0.44	45
0.15	62 ± 12	0.49	125	0.42	44
0.2	61 ± 13	0.44	119	0.42	38
0.4	60 ± 13	0.40	115	0.44	33

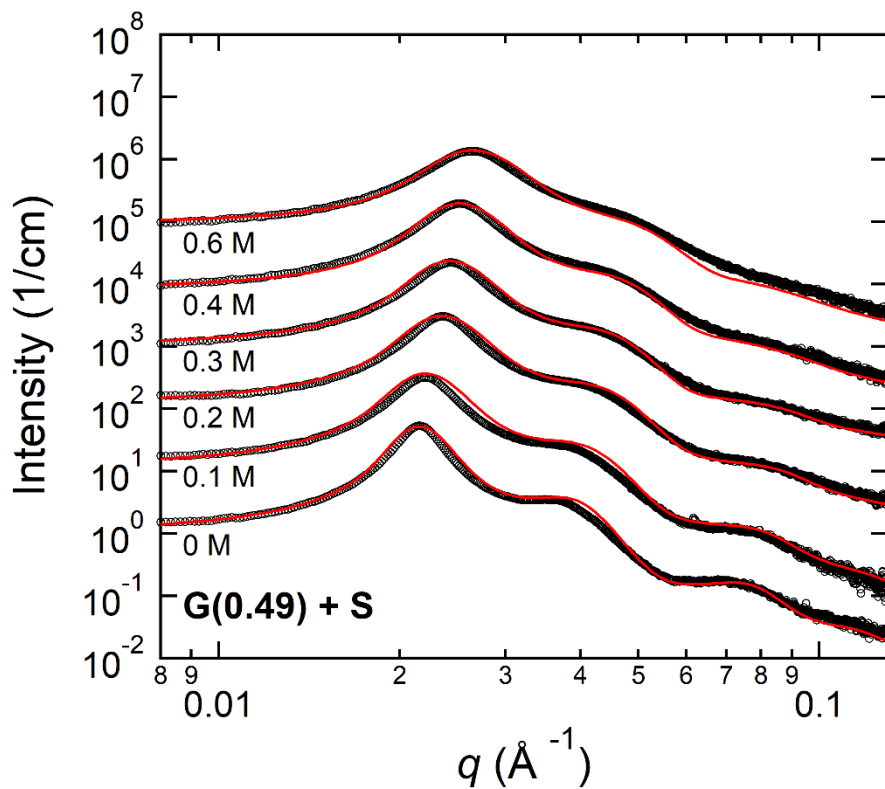


Figure S6. SAXS profiles obtained from $G_{0.49} + S$ hydrogels at various c_{NaCl} . Red solid lines denote the model fitting.

Table S8. Structural parameters obtained from SAXS of the $G_{0.49} + S$ hydrogels.

c_{NaCl} [M]	R_{core} [Å]	φ_{P} [-]	R_{hs} [Å]	η_{hs} [-]	N_{agg} [-]
0	74 ± 9	0.51	156	0.49	72
0.1	71 ± 9	0.51	148	0.47	65
0.2	67 ± 11	0.49	137	0.46	53
0.3	66 ± 11	0.47	133	0.45	49
0.4	65 ± 12	0.44	128	0.45	44
0.6	62 ± 12	0.40	116	0.42	35

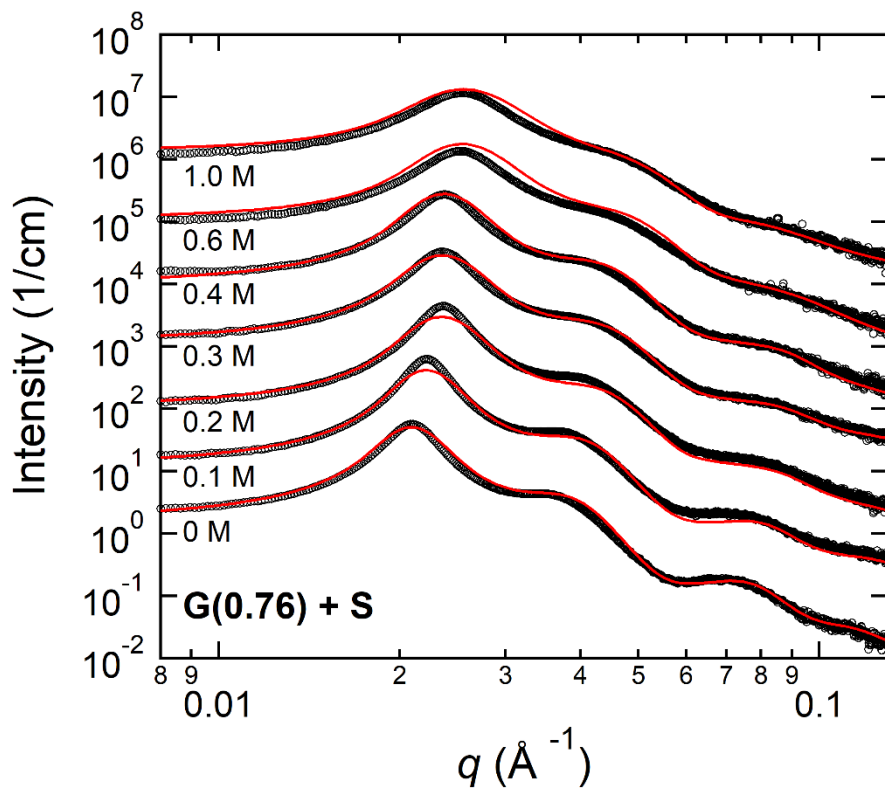


Figure S7. SAXS profiles obtained from $G_{0.76} + S$ hydrogels at various c_{NaCl} . Red solid lines denote the model fitting.

Table S9. Structural parameters obtained from SAXS of the $G_{0.76} + S$ hydrogels.

c_{NaCl} [M]	R_{core} [Å]	φ_{P} [-]	R_{hs} [Å]	η_{hs} [-]	N_{agg} [-]
0	75 ± 9	0.55	158	0.46	79
0.1	70 ± 9	0.56	150	0.47	66
0.2	66 ± 11	0.52	138	0.46	53
0.3	65 ± 11	0.54	136	0.45	52
0.4	65 ± 11	0.53	136	0.46	51
0.6	63 ± 11	0.48	125	0.43	43
1.0	62 ± 12	0.46	118	0.39	40

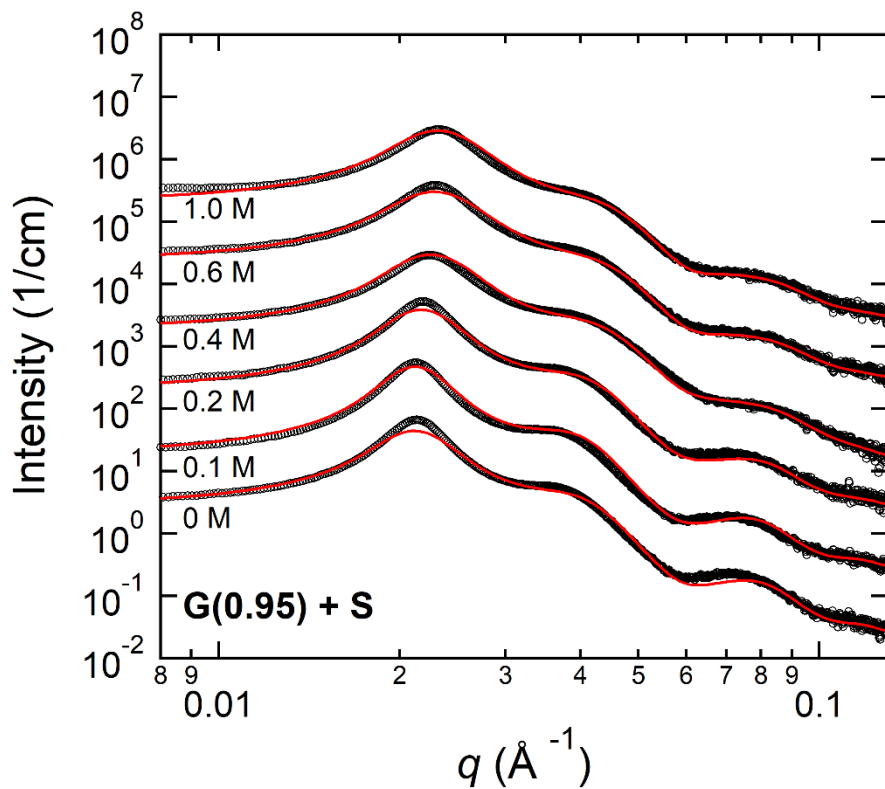


Figure S8. SAXS profiles obtained from $G_{0.95} + S$ hydrogels at various c_{NaCl} . Red solid lines denote the model fitting.

Table S10. Structural parameters obtained from SAXS of the $G_{0.95} + S$ hydrogels.

c_{NaCl} [M]	R_{core} [Å]	φ_{P} [-]	R_{hs} [Å]	η_{hs} [-]	N_{agg} [-]
0	72 ± 8	0.62	151	0.41	77
0.1	73 ± 8	0.59	155	0.45	76
0.2	71 ± 9	0.58	148	0.43	70
0.4	68 ± 11	0.56	139	0.41	60
0.6	67 ± 11	0.57	134	0.37	59
1.0	66 ± 11	0.56	128	0.35	56

Scaling Models and Interfacial Tensions

The free energy penalties per chain by the excluded volume interactions in the corona domain (F_{corona}) and the stretching of Gaussian chains in the core domain (F_{core}) were evaluated to determine whether the present system is closer to the hairy micelle model or the crew-cut micelle model. Both were calculated using the expressions developed from Ref. 12:

$$F_{\text{corona}}/k_{\text{B}}T = (1/2)N_{\text{agg}}^{1/2}\ln(R_{\text{hs}}/R_{\text{c}}) \quad (\text{S12})$$

and

$$F_{\text{core}}/k_{\text{B}}T = (3\pi^2/80)R_{\text{c}}^2/a^2N_{\text{core}} \quad (\text{S13}),$$

where $a = 0.6$ nm was used as the monomer size for the core block. Figure S9 summarizes the estimated free energies from all C3G samples and displays that F_{corona} is generally more than two times larger than F_{core} . Therefore, F_{core} is ignored to calculate the free energy balance for micellization.

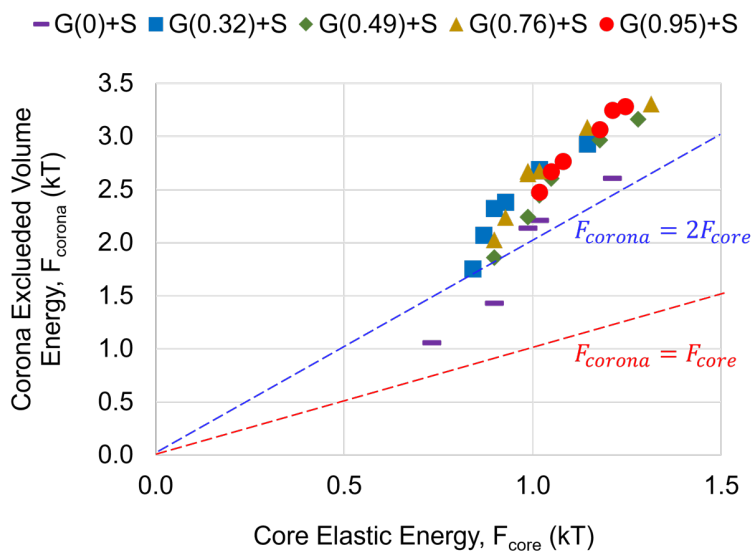


Figure S9. The free energy per chain due to the excluded volume effect in the corona, F_{corona} , versus the free energy per chain due to the core block stretching, F_{core} . The energies are expressed in unit of thermal energy, $k_{\text{B}}T$. The dashed lines serve as guides to compare the magnitudes of F_{corona} and F_{core} .

Table S11. Zero-salt interfacial tension and critical salt concentration from the fitting model. Interfacial tension was rescaled using the reference value of 1.4 mN/m for $G_0 + S$.

Sample code	g_0 [-]	γ_0 [mN/m]	c^* [mol/L]
$G_0 + S$	10.7	1.68	0.70
$G_{0.32} + S$	12.2	1.96	1.08
$G_{0.49} + S$	13.7	2.20	1.54
$G_{0.76} + S$	14.4	2.31	2.32
$G_{0.95} + S$	15.3	2.45	4.50

References

- (1) Roe, R. J. *Methods of X-Ray and Neutron Scattering in Polymer Science*; Oxford University Press: New York, 2000.
- (2) Efimova, Y. M.; van Well, A. A.; Hanefeld, U.; Wierczinski, B.; Bouwman, W. G. On the Neutron Scattering Length Density of Proteins in H₂O/D₂O. *Phys. B-Condensed Matter* **2004**, *350*, E877–E880.
- (3) Li, L.; Srivastava, S.; Andreev, M.; Marciel, A. B.; de Pablo, J. J.; Tirrell, M. V. Phase Behavior and Salt Partitioning in Polyelectrolyte Complex Coacervates. *Macromolecules* **2018**, *51*, 2988–2995.
- (4) Perkins, S. J. Protein Volumes and Hydration Effects. *Eur. J. Biochem.* **1986**, *157*, 169–180.
- (5) Vidulich, G. A.; Evans, D. F.; Kay, R. L. The Dielectric Constant of Water and Heavy Water between 0 and 40 Degree. *J. Phys. Chem.* **1967**, *71*, 656–662.
- (6) Krezel, A.; Bal, W. A Formula for Correlating PKa Values Determined in D₂O and H₂O. *J Inorg Biochem* **2004**, *98*, 161–166.
- (7) Wade, D. Deuterium Isotope Effects on Noncovalent Interactions between Molecules. *Chem. Biol. Interact.* **1999**, *117*, 191–217.
- (8) Pedersen, J. S.; Svaneborg, C.; Almdal, K.; Hamley, I. W.; Young, R. N. A Small-Angle Neutron and X-Ray Contrast Variation Scattering Study of the Structure of Block Copolymer Micelles: Corona Shape and Excluded Volume Interactions. *Macromolecules* **2003**, *36*, 416–433.
- (9) Ortony, J. H.; Choi, S.-H.; Spruell, J. M.; Hunt, J. N.; Lynd, N. A.; Krogstad, D. V; Urban, V. S.; Hawker, C. J.; Kramer, E. J.; Han, S. Fluidity and Water in Nanoscale Domains

- Define Coacervate Hydrogels. *Chem. Sci.* **2014**, *5*, 58–67.
- (10) Heo, T. Y.; Kim, I.; Chen, L. W.; Lee, E.; Lee, S.; Choi, S. H. Effect of Ionic Group on the Complex Coacervate Core Micelle Structure. *Polymers (Basel)*. **2019**, *11*.
- (11) Bang, J.; Viswanathan, K.; Lodge, T. P.; Park, M. J.; Char, K. Temperature-Dependent Micellar Structures in Poly(Styrene-*b*-Isoprene) Diblock Copolymer Solutions near the Critical Micelle Temperature. *J. Chem. Phys.* **2004**, *121*, 11489–11500.
- (12) Zhulina, E. B.; Borisov, O. V. Theory of Block Polymer Micelles: Recent Advances and Current Challenges. *Macromolecules* **2012**, *45*, 4429–4440.